Acetylated African Oil Bean Seed Pod For Crude Oil Spill Mop

Amalachukwu Ifeyinwa Obi (ai.obi@unizik.edu.ng)
Nnamdi Azikiwe University https://orcid.org/0000-0003-1002-9248
Vincent Ishmael Ajiwe
Nnamdi Azikiwe University

Research Article

Keywords: Oil bean seed pod, Acetylation, Oil spill mop

Posted Date: January 5th, 2022

DOI: https://doi.org/10.21203/rs.3.rs-1220132/v1

ACETYLATED AFRICAN OIL BEAN SEED POD FOR CRUDE OIL SPILL MOP

Amalachukwu I. Obi* and Vincent I. Ajiwe

*Correspondence: ai.obi@unizik.edu.ng

Department of Pure and Industrial Chemistry, Nnamdi Azikiwe University, Awka, Anambra State, Nigeria.

ABSTRACT

Oil spill remediation has continued to be a challenge in the world today. Thus efforts are still been made to develop more efficient oil spill mop up techniques. Natural adsorption with agricultural wastes, which otherwise constitute environmental pollution, has become an attractive technique for oil spill mop. Acetylation using acetic anhydride with iodine catalyst was carried out to improve the hydrophobicity of African oil bean seed pod (AOBSP), which is a lignocellulosic material and as such is naturally hydrophilic. Characterization of the raw and acetylated AOBSP were done using SEM, BET and FTIR analyses. Batch crude oil sorption tests were performed using both the raw and acetylated AOBSP. Isotherm, kinetic and thermodynamic studies were also carried out. FTIR analysis showed evidence of successful acetylation of AOBSP and adsorption of crude oil onto the raw and acetylated AOBSP. SEM and BET analyses showed improvement of the surface properties of AOBSP by the acetylation process. The BET surface area increased from 226.4 m^2/g for the raw AOBSP to 310.0 m^2/g for the acetylated AOBSP. Oil sorption was found to be by monolayer coverage, with monolayer sorption capacity of 5000mg/g and 12500mg/g for raw and acetylated AOBSP, respectively. The rate-controlling mechanism for the sorption processes was chemisorption. Negative values of ΔG^o, ΔH^o and ΔS^o were obtained, showing that the sorption processes were feasible, spontaneous and exothermic, with a degree of orderliness at the solid–mixture interface. The results obtained from this study show that both raw and acetylated AOBSP are efficient oil sorbents with potentials for further improvement for oil spill mop.

Keywords: Oil bean seed pod, Acetylation, Oil spill mop

INTRODUCTION

Environmental pollution due to crude oil spillage occurs during the various stages of its extraction, transportation, refining, storage, and use. Up to 100 million gallons of crude oil have been estimated to spill into marine environments each year (Barros et al. 2014). This causes adverse effects on aquatic life, human life, local economies, tourism, as well as leisure activities (Wali et al. 2019). Thus, so many efforts are being made towards the development of a very suitable means of oil spill remediation. Many mechanical, biological, chemical and adsorption technologies are been used for removal of oil spills in aqueous environments. However, natural adsorption method using low cost agricultural materials and wastes is a preferred method because of its simplicity, low cost, effectiveness as well as availability, renewability and biodegradability of the sorbents (Xu et al. 2018). These wastes themselves, as well as their disposal usually constitute environmental concerns (Li et al. 2021). Thus, their conversion into valuable products will aid in providing solution to environmental pollution. The major snag with the use of agricultural materials and wastes in oil spill mop is the hydrophilic nature of the materials (Omer et al. 2020), which is as a result of their high hydroxyl content (Anuzyte and Vaisis, 2018). This can, however, be addressed by modification processes which confer hydrophobic properties to the materials (Thompson et al. 2015). Acetylation is one of the most commonly used modification methods, and it changes the hydrophilic nature of lignocellulosic materials to hydrophobic by replacing some of their hydroxyl (–OH) groups with acetyl groups ($–COCH_3$), which are hydrophobic (Onwuka et al. 2019). Acetylation of various agricultural materials such as corn silk (Asadpour et al., 2015), jute fibre (Teli and Valia 2016), corn cob (Nwadiogbu et al. 2016), cocoa pods and oil palm fruit empty bunch (Onwuka et al. 2018) have been carried out in order to improve their oil sorption capacity.

African oil bean seed pod is a readily available, biodegradable waste obtained from the African oil bean tree (*Pentaclethra macrophylla*). It usually falls off from the tree after splitting open to expel the

seeds which are highly nutritious and usually consumed as food condiment or snack after fermentation or roasting (Nwosu et al. 2017). The empty dry pods are not useful and usually constitute environmental pollution. Studies have been carried out on its use for production of activated carbon (Aningo et al. 2017) and adsorption of heavy metals (Okwunodulu et al. 2015). However, its acetylation for improvement of crude oil sorption potential has not yet been studied.

METHODS

The crude oil used in this work was collected from Port Harcourt Refinery Rivers State, Nigeria. African oil bean seed pods (AOBSP) were collected from Awka environment in Anambra State, Nigeria. They were thoroughly washed with clean water to remove dust and extraneous materials. Then they were dried under sunlight for 12 hours, and then transferred to an oven at 65ºC to dry completely. The dried samples were ground using manual grinding machine and sieved. The particles that passed through size 25 British standard sieves (BSS Sieves) were collected and used for further analyses. Acetic anhydride, iodine and all other chemicals used in this work were obtained from British Drug Houses, Ltd.

Crude oil characterization

The density of the crude oil was determined using the density bottle method as reported by Oloro (2018). The ^{o}API gravity was obtained using the formula for API (American Petroleum Institute) gravity as expressed by Al-Dahhan and Mahmood (2019). The viscosity of the crude oil was obtained using an NDJ-85 Digital rotary viscometer at 27^{o}C.

Soxhlet extraction

In order to reduce the influence of fiber extracts on acetylation, soxhlet extraction was carried out on the AOBSP. For this, 10g of the sieved materials were extracted with a mixture of n-hexane and acetone (4:1, v/v) for 5 hours. The extracted samples were dried in a laboratory oven for 16 hours.

73 **Acetylation reaction**

74 Acetylation of AOBSP was carried out under mild conditions using the method reported by Nwabueze
75 et al. (2005) which involved acetylation without solvent. A weighed portion (3g) of the AOBSP was
76 reacted with acetic anhydride (60mL) in the presence of 1% iodine catalyst at 30ºC for 1 hour. The
77 acetylated samples were then dried in an oven at 60ºC for 16 hours, after which they were cooled and
78 stored for further analysis.

79 **Sorbent characterization**

80 Fourier-Transform Infrared (FTIR) spectra was collected using a Nicolet iS5 spectrometer in the
81 spectral range of 4000-400cm^{-1} in attenuated total reflection (ATR) mode. This was used to identify
82 the functional groups present in the raw and acetylated AOBSP. The surface morphologies of the raw
83 and acetylated AOBSP were observed using Phenom ProX Scanning Electron Microscope by
84 PhenomWorld Eindhoven, the Netherlands. The surface area, pore volume and size were determined
85 using BET analyzer (Quantachrome NOVA 4200e).

86 **Crude oil adsorption**

87 Crude oil for the sorption test was left in a beaker for 24 hours in open air to release volatile
88 hydrocarbon contents, and thus simulate real oil spill situation. Batch sorption tests were carried out
89 using the method described by Nwadiogbu et al. (2016) by contacting 0.2g each of the raw and
90 acetylated AOBSP with 10g of the weathered crude oil displaced in 100 mL of water at 26ºC. After
91 15mins the sorbents were removed using sieving nets and dried at 60ºC for 30minutes, after which they
92 were re-weighed. Oil sorption capacity (g/g) was calculated according to the standard method (ASTM
93 F726-99) as shown in Equation 1.

94 $$\text{Oil sorption capacity} = \frac{W_1 - W_0}{W_0} \qquad (1)$$

where W_0 and W_1 are the weight of adsorbent before and after oil adsorption, respectively, and the quantity $W_1 - W_0$ is the amount of crude oil adsorbed in grams. The amount of crude oil adsorbed per unit weight of adsorbent, q_e (mg/g), was calculated using Equation 2.

$$q_e = \frac{(C_o - C_e)V}{m} \quad (2)$$

where C_o is the initial crude oil concentration (mg/L), C_e is the equilibrium crude oil concentration (mg/L), m is the mass of the adsorbent (g) and V is the volume of the solution (L).

Kinetic study

Three well known kinetic models were employed to study the kinetics of the oil adsorption. These are the pseudo first order, pseudo second order and intraparticle diffusion models.

The pseudo first order kinetic model

The linearized pseudo first order equation is as shown in Equation 3 (Ho and McKay, 2000).

$$\ln (q_e - q_t) = \ln q_e - k_1 t \quad (3)$$

where q_e is the amount of adsorbate adsorbed at equilibrium (mg/g), q_t is the amount of adsorbate adsorbed in mg/g at time t (min), and k_1 is the pseudo first order reaction rate constant (min^{-1}). A plot of $\ln (q_e - q_t)$ versus t gives a straight line graph yielding k_1 and q_e from its slope and intercept, respectively.

The pseudo second order kinetic model

The linearized pseudo second order equation is as expressed in Equation 4 (Ofomaja and Ho, 2007).

$$\frac{t}{q_t} = \frac{1}{k_2 . q_e^2} + \frac{t}{q_e} \quad (4)$$

where q_e and q_t are the sorption capacity (mg/g) at equilibrium and at time t (min), respectively, and k_2 is the pseudo-second order reaction rate constant (g/mg.min). A plot of t/q_t versus t should give a linear relationship, from which q_e and k_2 can be determined from the slope and intercept of the plot, respectively.

Intraparticle diffusion model

The intraparticle diffusion model is expressed in Equation 5 (Idris et al. 2012).

$$q_t = K_{id}\, t^{0.5} + C \qquad (5)$$

where K_{id} is the rate constant of intraparticle diffusion (mg/(g·min$^{0.5}$)), $t^{0.5}$ is the square root of the time, and C is the intercept.

Isotherm study

Two popular isotherms were used to study the equilibrium of the oil adsorption process. They are Langmuir isotherm and Freundlich isotherm.

Langmuir isotherm

The linearized Langmuir isotherm is expressed in Equation 6 (Santos et al. 2015).

$$\frac{C_e}{q_e} = \frac{1}{K_L.q_m} + \frac{C_e}{q_m} \qquad (6)$$

where q_m is the maximum monolayer adsorption capacity (mg/g) and K_L (L/mg) is the Langmuir or equilibrium constant of adsorption which is a measure of affinity of the adsorbate for the adsorbent and is related to the energy of sorption. A plot of $\frac{C_e}{q_e}$ against C_e yields a straight line graph whose slope and intercept can be used to determine q_m and k_L, respectively. A dimensionless constant called the separation factor or equation parameter, R_L, which is expressed in Equation 7 (Gupta et al. 2001) is used to predict the affinity between an adsorbent and adsorbate.

$$R_L = \frac{1}{1 + k_L.C_o} \qquad (7)$$

where, C_o is the initial adsorbate concentration. The value of R_L indicates the adsorption nature to be unfavorable if $R_L>1$, linear if $R_L=1$, favorable if $0<R_L<1$ and irreversible if $R_L=0$.

Freundlich isotherm

The linearized Freundlich equation is expressed in Equation 8 (Shah et al. 2021).

$$\ln q_e = \ln K_F + \frac{1}{n} \ln C_e \quad (8)$$

where, K_F [(mg/g)/(mg/L)$^{1/n}$] is the Freundlich constant, which indicates the relative adsorption capacity of the adsorbent, and n is a measure of the adsorption intensity showing the heterogeneity of the adsorbent site and the energy of distribution. The values of K_F and n are determined from the intercept and slope, respectively, of a linear plot of ln q_e as a function of ln C_e. Values of n between 1 and 10 indicate favourable adsorption (Karthikeyan *et al*., 2003).

Thermodynamic studies

The standard Gibbs free energy changes for the adsorption processes was determined using van't Hoff equation as shown in Equation 9 (Li et al. 2009).

$$\Delta G^o = -RT \ln K_d \quad (9)$$

where ΔG^o is the free energy change (kJ/mol), R is the universal constant (8.314J/mol.K), T is the absolute temperature (K), and K_d is distribution coefficient for the adsorption (cm^3/g). K_d was calculated using Equation 10.

$$K_d = \frac{C_s}{C_e} \quad (10)$$

where C_s is the amount of adsorbate adsorbed on the sorbent at equilibrium.

The changes in enthalpy, ΔH^o (kJ/mol), and entropy, ΔS^o (kJ/mol.K) were calculated using Equation 11 (Babarinde et al. 2016).

$$\Delta G^o = \Delta H^o - T\Delta S^o \quad (11)$$

A plot of ΔG^o versus T gives a straight line graph from whose slope and intercept ΔS^o and ΔH^o are obtained, respectively.

RESULTS AND DISCUSSION

The characterizing properties of the crude oil are shown in Table 1.

Table 1: Crude oil characterization

Parameter	Value
Density (kg/m^3)	876
^{o}API gravity	25.897
Viscosity (mPa.s)	3.958

The crude oil is less dense than water and so floats on water. It belongs to the class of medium crudes since its density is within the range of 870 - 920 kg/m^3 (Awadh and Al-Mimar, 2015) and the ^{o}API gravity is in the range of 22.3 - 31.1^o (Yasin et al. 2013). This implies that the crude oil has a blend of light and heavy oils (Madu and Ugwu, 2017).

Surface Morphology Identification

The SEM images of the raw and acetylated AOBSP are shown in Figures 1 and 2, respectively.

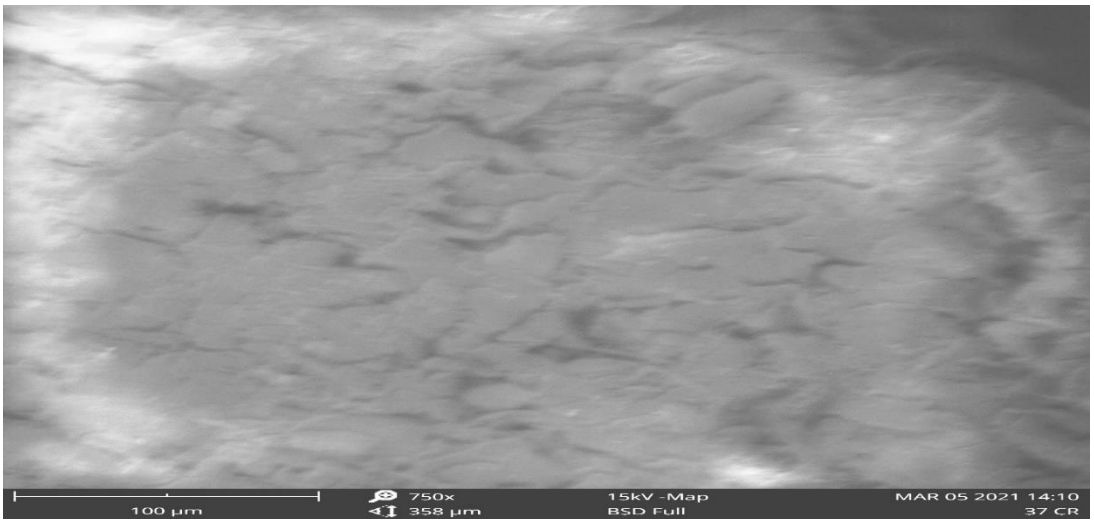

Figure 1: SEM micrograph of raw AOBSP

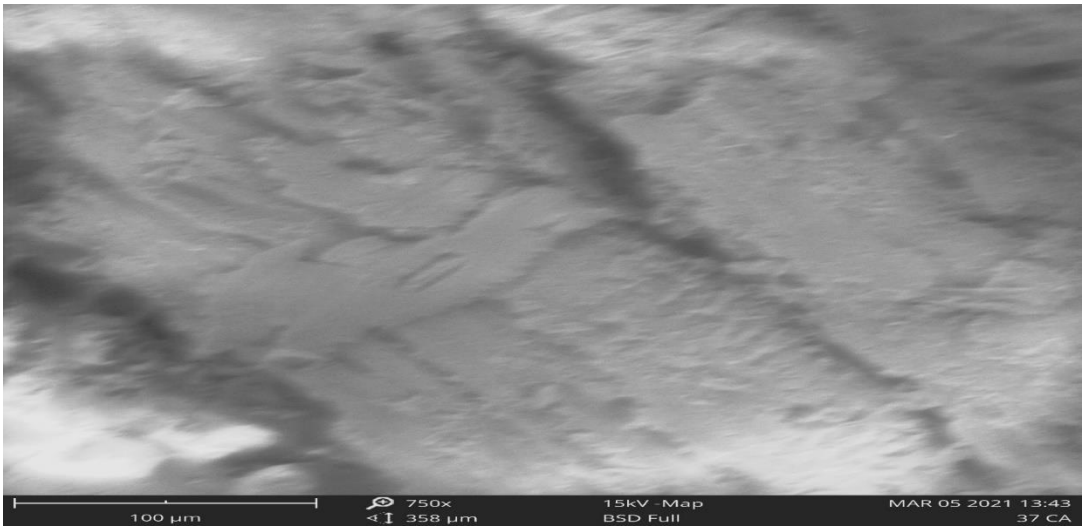

Figure 2: SEM micrograph of acetylated AOBSP

Acetylation increased the roughness and folds of the raw AOBSP surface, with formation of hollow structures. Similar observation was made by Asadpour et al. (2015) for the acetylation of corn silk. This change in morphology is due to the removal of weak constituents of hemicelluloses and lignin from the AOBSP structure by the acetylating agent (Mahmoud, 2020). This is desirable since it provides more spaces for the retention of oil in the sorbent, thus improving oil sorption and storage (Yusof et al. 2015).

Surface Area Measurements

The results of surface area, pore volume and pore size of the raw AOBSP are shown in Appendix 1A – 1J while for acetylated AOBSP they are shown in Appendix 2A – 2J. The results are summarized in Table 2. According to the International Union of Pure and Applied Chemistry, pore sizes are classified into three groups, which are micropores (diameter less than 20 Å or 2nm), mesopores (diameter between 20 Å or 2nm and 500 Å or 50nm), and macropores (diameter greater than 500 Å or 50 nm) (Asadpour et al. 2014). The pore size/diameter of the raw and acetylated AOBSP were in the same range and belonged to the mesopore group. Acetylation was found to substantially increase the surface area and pore volume of AOBSP. These increments are likely due to the formation of hollow structures

and increased roughness and folds of the raw AOBSP surface, as observed in SEM analysis. This is favorable since high active surface area results in high oil adsorption capacity (Angelova et al. 2011).

4.3 Fourier Transform Infra-red spectroscopy (FTIR)

The FTIR spectra for raw and acetylated AOBSP, before and after crude oil sorption, are shown in Figures 3 - 6, respectively. The assignment of functional groups are shown in Table 3.

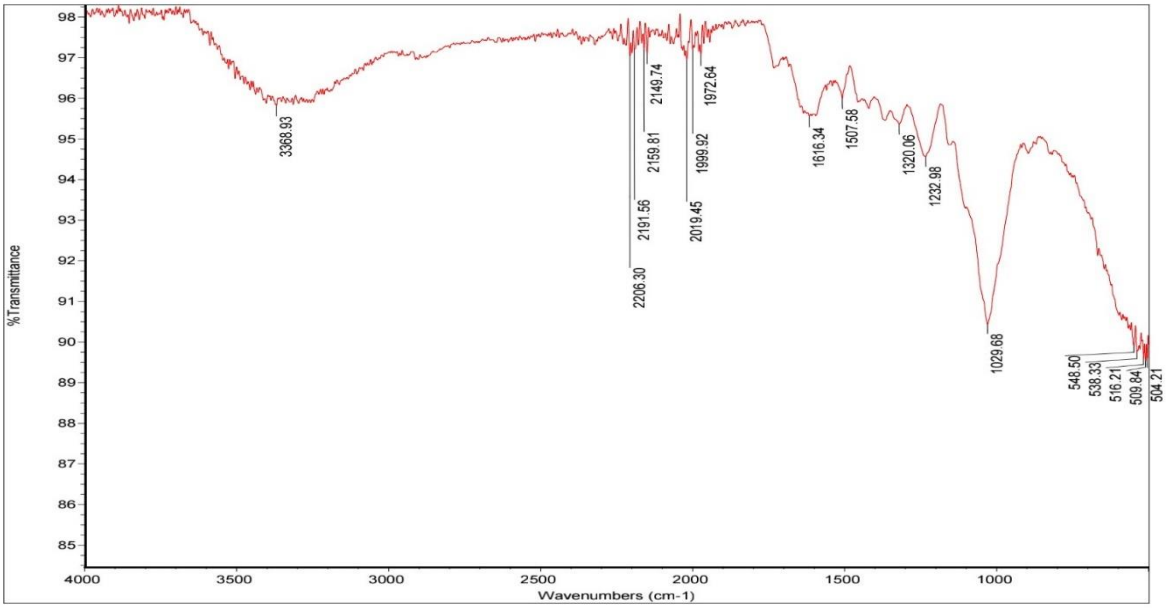

Figure 3: FTIR spectrum of raw African oil bean seed pod (RAOBSP)

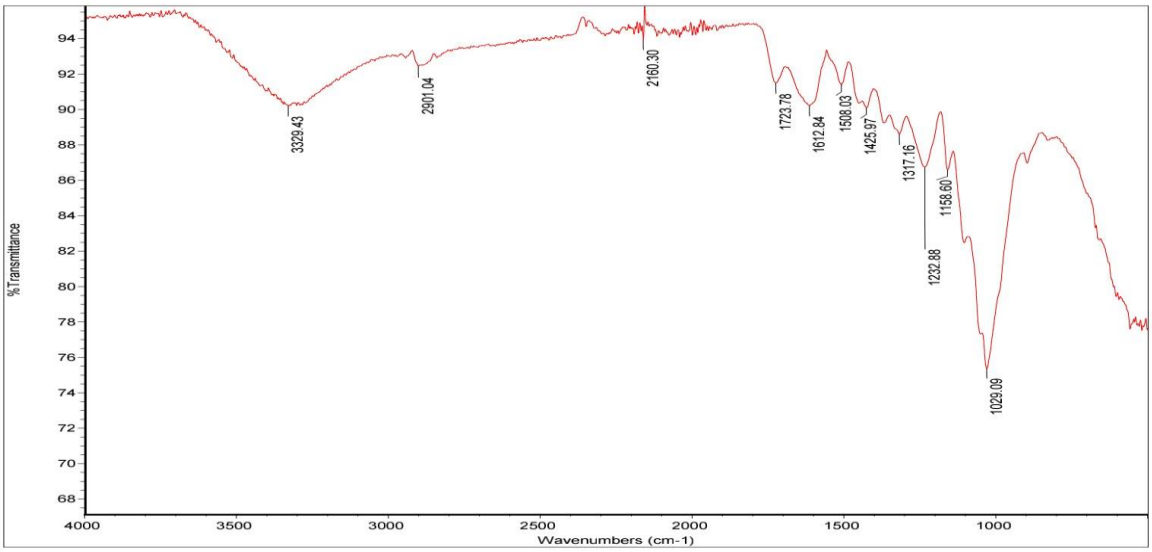

Figure 4: FTIR spectrum of acetylated African oil bean seed pod (AAOBSP)

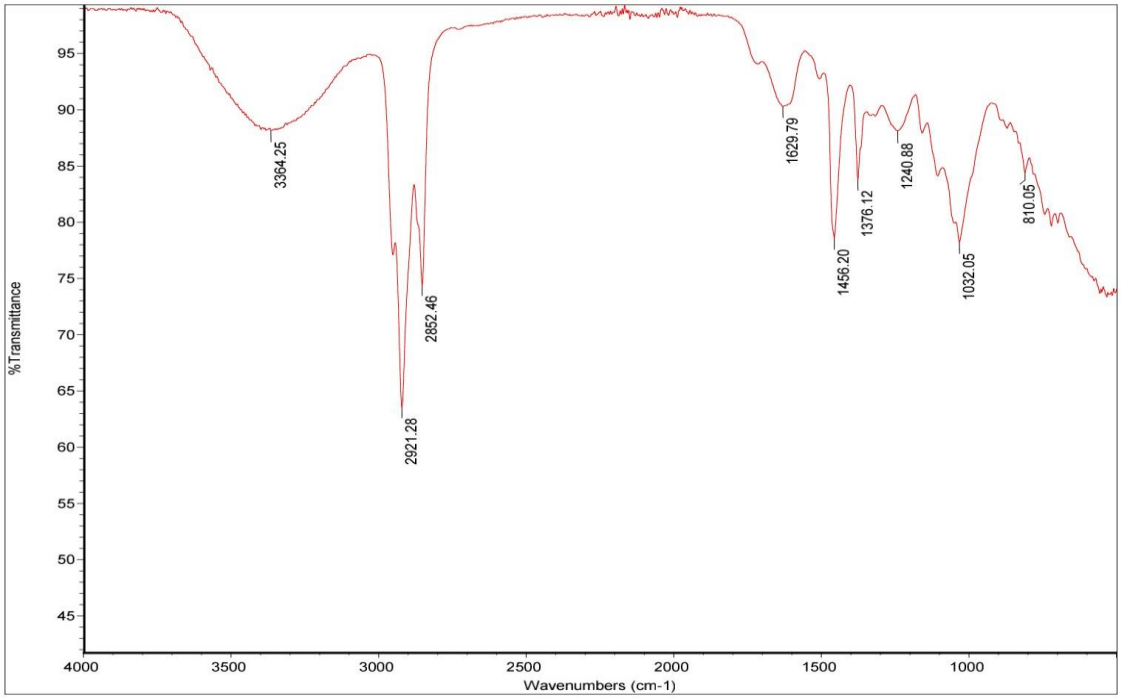

201

202 **Figure 5: FTIR spectrum of raw African oil bean seed pod after sorption (RAOBSP-S)**

203

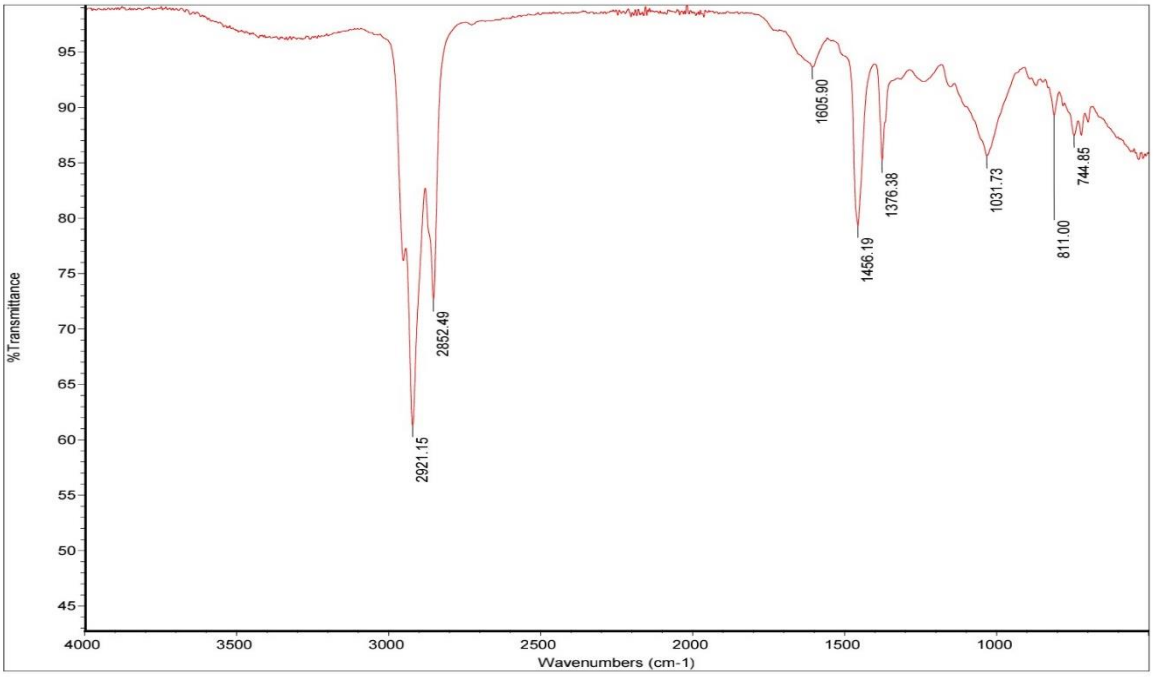

204

205 **Figure 6: FTIR spectrum of acetylated African oil bean seed pod after sorption (AAOBSP-S)**

206 **Table 3: FTIR bands of AOBSP and the corresponding functional groups**

RAOBSP (cm^{-1})	AAOBSP (cm^{-1})	RAOBSP-S (cm^{-1})	AAOBSP-S (cm^{-1})	Assignment
3368.93	3329.43	3364.25	-	O–H stretching in cellulose and hemicellulose
-	2901.04	2921.28	2921.15	C–H stretching of methyl and methylene groups
2191.56	2160.30	2852.46	2852.49	Cyanide ion stretching
1616.34	1723.78 1612.84	1629.79	1605.90	C=O stretching vibration
1507.58	1508.03	-	-	C=C stretching of aromatic ring
1320.06	1425.97 1317.16	1456.20 1376.12	1456.19 1376.38	C–H bending
1232.98 1029.68	1232.88 1158.60 1029.09	1240.88 1032.05	1032.71	C–O stretching vibration
-	-	810.05	810.75	C–H bending of β glycosidic bond
548.50 to 504.21	534.12 to 516.32	-	744.63	C–H out of plane bending

207 **Note: RAOBSP is raw AOBSP; AAOBSP is acetylated AOBSP; RAOBSP-S is raw AOBSP after**
208 **crude oil sorption; and AAOBSP-S is acetylated AOBSP after crude oil sorption.**

A comparison of the spectra of RAOBSP and AAOBSP shows the following major differences: creation of absorption peak at 2901.04 cm^{-1} (C–H stretching), enhancement of absorption peaks at 1612.84 – 1723.78 cm^{-1} (C=O stretching) and at 1029cm^{-1} (C–O stretching). These show evidence of acetylation of AOBSP (Onwuka et al. 2016). The lack of peaks at 1700 cm^{-1} (carboxylic group) and in the region of 1760-1840 cm^{-1} in the spectra of the acetylated sample indicates that the product was free of acetic acid byproduct and unreacted acetic anhydride (Bodîrlău and Teacă, 2009).

The spectra of the crude oil-treated sorbents show the appearance of intense sharp peaks at 2921cm^{-1}, 2852 cm^{-1} and 1376.12 – 1456.40 cm^{-1} which correspond to CH_3, CH_2 and C-H bending of crude oil showing that crude oil was adsorbed to the adsorbents (Kudaybergenov et al. 2013). These peaks are found to be more intense in AAOBSP-S than RAOBSP-S showing that the acetylated sample adsorbed more crude oil than the raw sample. The spectra of AAOBSP-S shows absence of peak at 3329.43 – 3368.93cm^{-1} (O–H stretching), as well as reduced peaks at 1029.09 – 1232.98cm^{-1} (C–O stretching) and 1605.63 – 1629.79cm^{-1} (C=O stretching). This may indicate the involvement of these groups in the adsorption of crude oil to the acetylated sample (Shittu et al. 2020). The obtained FTIR spectra are consistent with those reported for crude oil adsorption by raw and acetylated corn silk (Asadpour et al. 2015) and Delonix *regia* pods (Onwuka et al. 2016).

Adsorption Studies

The effects of different parameters on the crude oil sorption capacity of both the raw and acetylated AOBSP were studied and the results are as follows.

Effect of contact time

The effect of contact time on crude oil sorption capacity of the raw and acetylated AOBSP is shown in Figure 7.

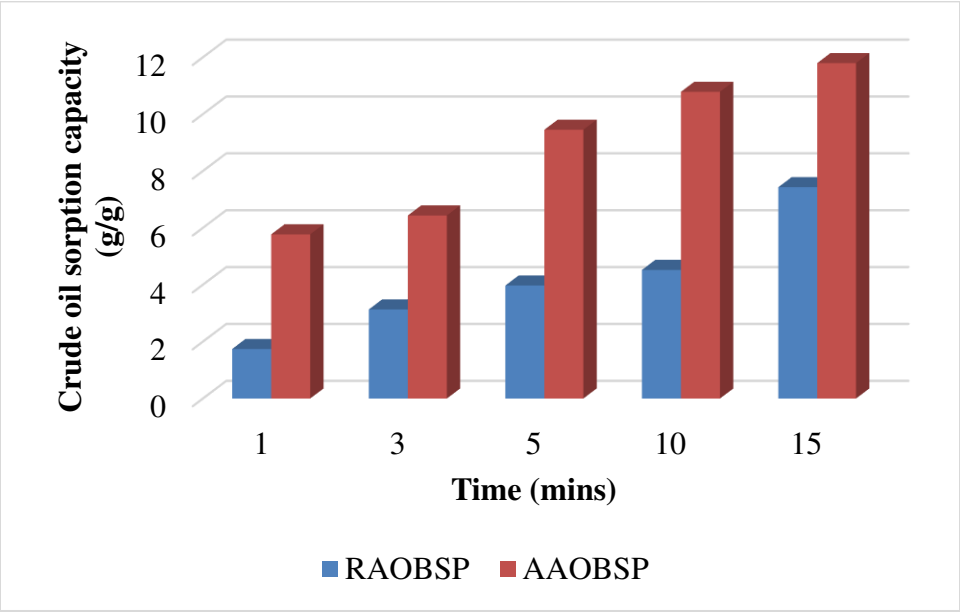

Figure 7: Effect of contact time on crude oil sorption capacity

The crude oil sorption capacity of the adsorbents was found to increase with increase in contact time from 1 to 15minutes. The sorption process was rapid at the initial stages of contact and thereafter it became slower towards equilibrium. This may be due to the fact that at the onset of contact, the high concentration gradient between the oil solution and the sorbent surface leads to high diffusion of oil into the pores of the sorbent. But, as time passed, the adsorbed oil started to clog the sorbent's pores and so oil could no longer diffuse to the active sites deep within the sorbent (Najaa-Syuhada et al. 2017). Similar trend was reported for crude oil adsorption on raw and acetylated *Borassus aethopum* coir by Arinze-Nwosu et al. (2019).

Throughout the adsorption period, the acetylated AOBSP had higher sorption capacity than the raw AOBSP. At 15minutes of contact time, the sorption capacities of the raw and acetylated AOBSP were 7.430 g/g and 11.795 g/g, respectively. The higher sorption capacity of the acetylated AOBSP is likely due to its higher surface area and pore volume, as observed in surface area analysis, which provides more spaces for oil adsorption. Increase in crude oil sorption capacity on acetylation was also reported by Onwuka et al. (2018) who found the crude oil adsorption capacity of raw and acetylated cocoa pods

247 to be 3.97 and 6.65 g/g, respectively, while raw and acetylated oil palm empty fruit bunch had values
248 of 3.04 and 6.48 g/g, respectively.

249 **Effect of temperature**

250 The effect of temperature on the crude oil sorption capacity of the raw and acetylated AOBSP is shown
251 in Figure 8.

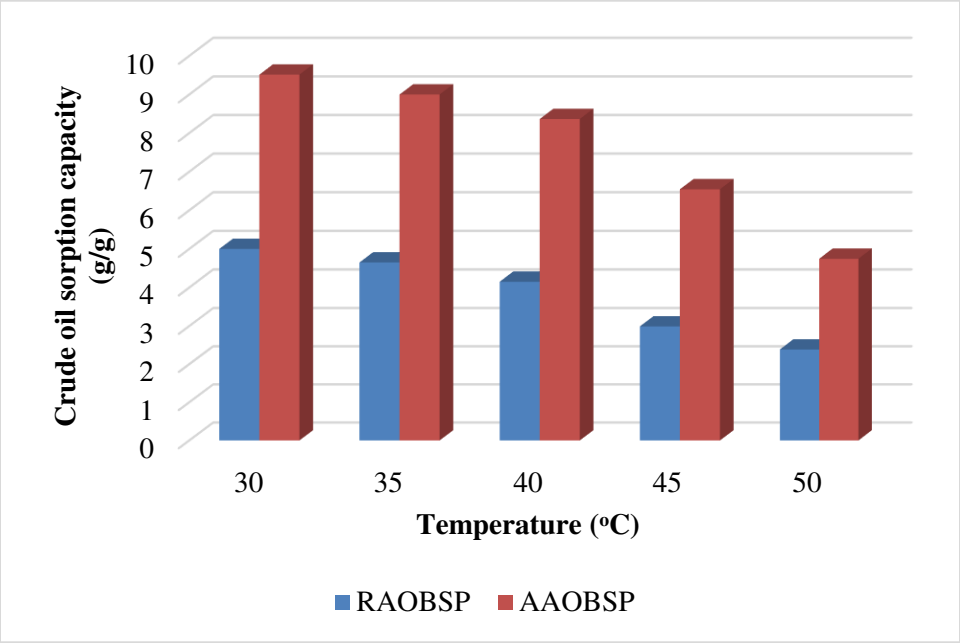

252

253 **Figure 8: Effect of temperature on crude oil adsorption capacity**

254 Crude oil sorption capacity decreased with increase in temperature from 30°C to 50°C. This may be
255 due to the fact that increase in temperature accelerates the Brownian motion of the oil molecules, thus
256 a stronger force is needed to keep the molecules adsorbed to the sorbent surface (Simonivić et al. 2009).
257 The decrease in the crude oil sorption capacity with increasing temperature also shows that the
258 adsorption process was exothermic in nature. Similar behaviour was reported by El-Din et al. (2018)
259 for the use of banana peels to adsorb 1-day and 7-day weathered crude oil. An increase in temperature
260 from 20 to 45°C resulted in decrease of sorption capacity of the sorbent from 7.94 g/g and 7.14g/g to
261 4.52 g/g and 3.25g/g for 1-day and 7-day weathered crude oil, respectively.

Effect of adsorbent dose

The effect of adsorbent dose on the crude oil sorption capacity of the raw and acetylated AOBSP is shown in Figure 9 while the effect of adsorbent dose on the amount of crude oil adsorbed is shown in Figure 10.

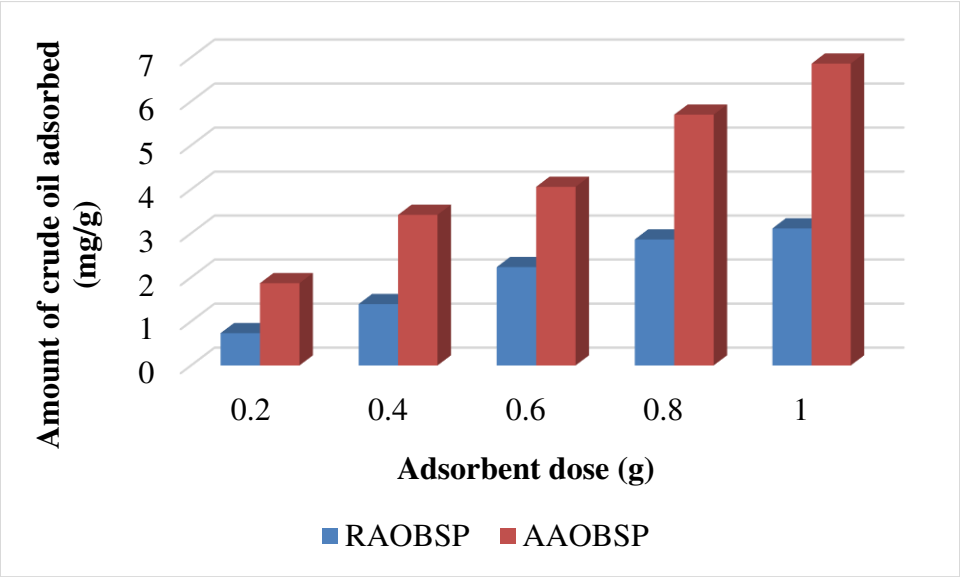

Figure 9: Effect of adsorbent dose on amount of crude oil adsorbed

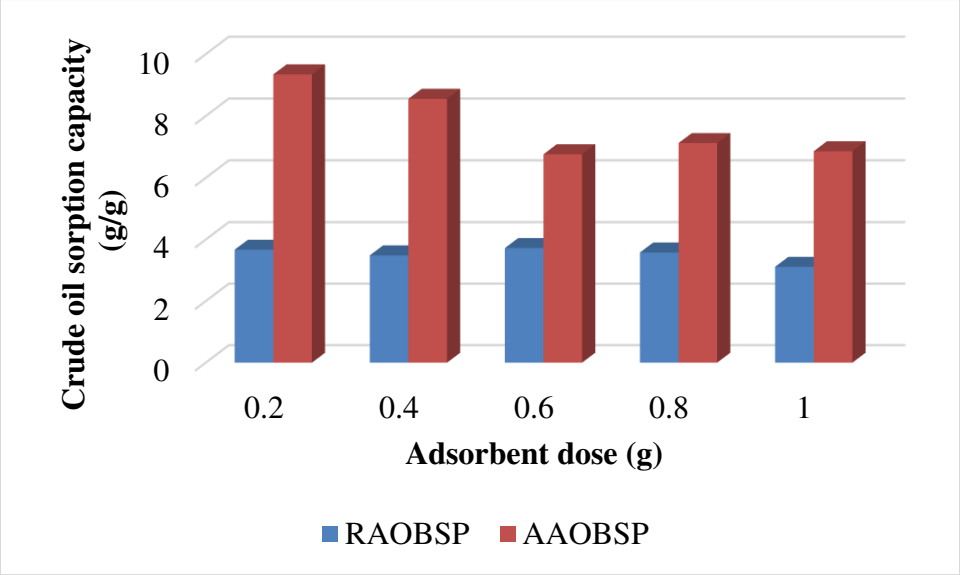

Figure 10: Effect of adsorbent dose on crude oil sorption capacity

As sorbent dose increased from 0.2g to 1g, amount of crude oil adsorbed on both the raw and acetylated AOBSP increased from 0.734mg/g to 3.113mg/g and 1.869mg/g to 6.860mg/g, respectively. This may be due to the fact that increase in quantity of adsorbent resulted in the availability of more surface area/active binding sites (Akinhanmi et al. 2020). However, as the sorbent dose increased, there was a general decrease in the crude oil sorption capacity of both the raw and acetylated AOBSP. This decrease may be due to the fact that as sorbent dose increases, sorption sites aggregate and overlap, thereby reducing total accessible surface area. This results in reduction of the quantity of sorbate adsorbed by a unit mass of sorbent, which leads to reduction of sorption capacity (Shweta and Jha 2016). Similar behaviour was reported by Nwadiogbu et al. (2016) who found the crude oil sorption capacity of raw and acetylated corn cob to decrease from 4000mg/g to 1000mg/g and 2300mg/g to 500mg/g, respectively on increasing the sorbent dosage from 0.5g to 2g.

Kinetic study

The pseudo first order, pseudo second order and intraparticle diffusion data for crude oil adsorption on raw and acetylated AOBSP are shown in Figures 11 – 13.

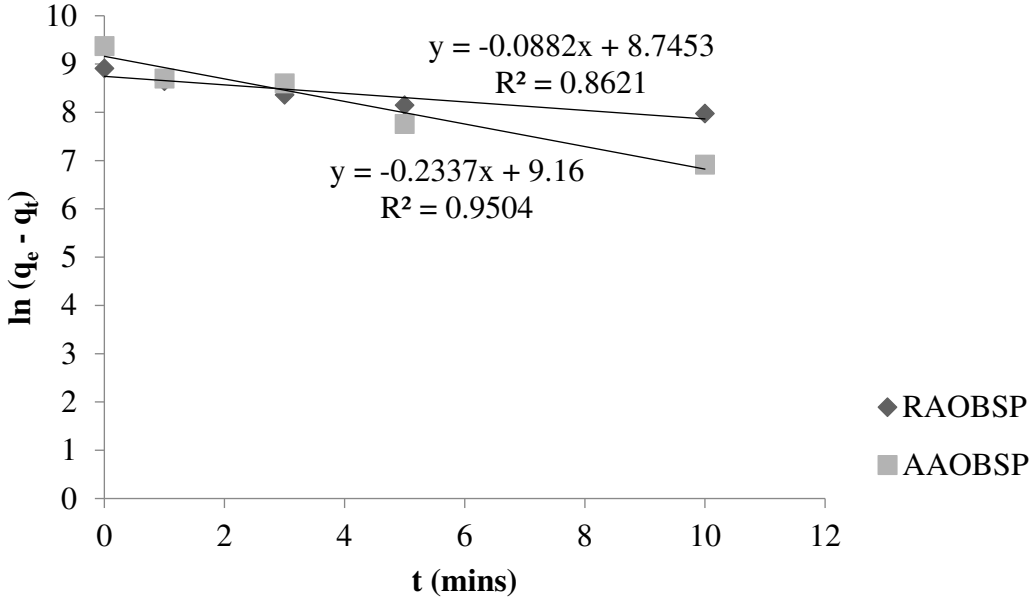

Figure 11: Pseudo first order kinetic plot

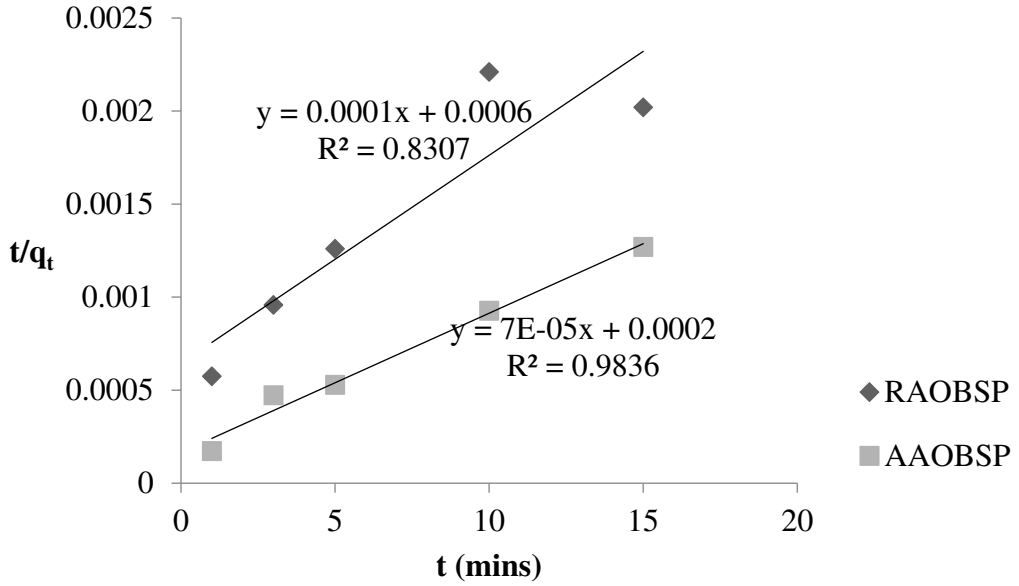

Figure 12: Pseudo second order kinetic plot

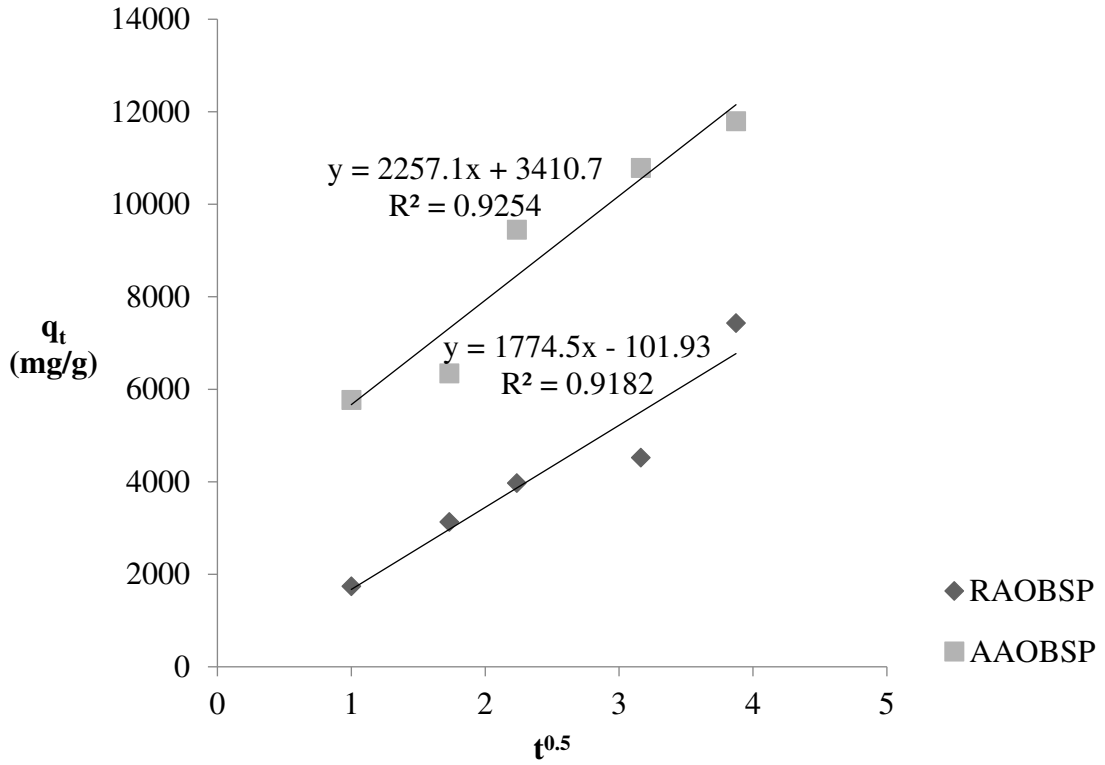

Figure 13: Intra particle diffusion kinetic plot

The kinetic parameters are shown in Table 4.

Table 4: Kinetic parameters for oil adsorption on raw and acetylated AOBSP

Parameter	RAOBSP	AAOBSP
$q_{e,}$ exp (mg/g)	7430	11795
Pseudo first order model		
R^2	0.8621	0.9504
k_1 (min^{-1})	0.0882	0.2337
$q_{e,}$ calc. (mg/g)	6281	9509
Pseudo second order model		
R^2	0.8307	0.9836
k_2 (min^{-1})	1.7×10^{-5}	2.5×10^{-5}
$q_{e,}$ calc. (mg/g)	10000	14286
Intraparticle diffusion model		
R^2	0.9182	0.9254
K_{id} ($mg/(g \cdot min^{0.5})$)	1774.5	2257.10
C	-101.93	3410.70

All the kinetic plots were found to be linear with high R^2 values (0.8307 - 0.9836). The pseudo-first, pseudo-second and intraparticle diffusion rate constants are higher for adsorption on acetylated AOBSP than on raw AOBSP. This suggests that physisorption, chemisorption as well as intraparticle diffusion of the crude oil was faster on acetylated AOBSP than on raw AOBSP, and this can be ascribed to the hydrophobicity of the acetylated AOBSP (Onwuka et al. 2016). The intra particle diffusion model graphs, though linear, did not pass through the origin. This shows that intra-particle diffusion took part in controlling the rate of oil sorption on both RAOBSP and AAOBSP, but it was not the sole mechanism (Thompson et al. 2015). The K_{id} value of AAOBSP was found to be higher than that of RAOBSP

showing that acetylation improved the adsorptive potential of AOBSP since higher K_{id} values indicate increase in the rate of adsorption as well as better adsorption mechanism (Erhan et al. 2004).

For adsorption on both raw and acetylated AOBSP, the pseudo-second order rate constant is lower than the pseudo-first order rate constant. This shows that chemisorption is the slowest step, and so is the rate-controlling step in the sorption process. This is supported by the fact that for adsorption on acetylated AOBSP, the pseudo-second-order R^2 value (0.9836) is higher than the pseudo-first-order R^2 value (0.9504). For adsorption on raw AOBSP the pseudo-first-order R^2 value (0.8621) is higher than the pseudo-second-order R^2 value. However, the pseudo-second-order value (0.8307) is also high and close to the pseudo-first-order value. Thus, it can be said that chemisorption is the rate-controlling mechanism in the sorption of oil on both raw and acetylated AOBSP, with physisorption being partly involved in the sorption process.

4.7.3 Isotherm studies

The Langmuir isotherms for crude oil adsorption on raw and acetylated AOBSP are shown in Figures 14 and 15, respectively, while the Freundlich isotherms are shown in Figures 16 and 17 for adsorption on raw and acetylated AOBSP, respectively.

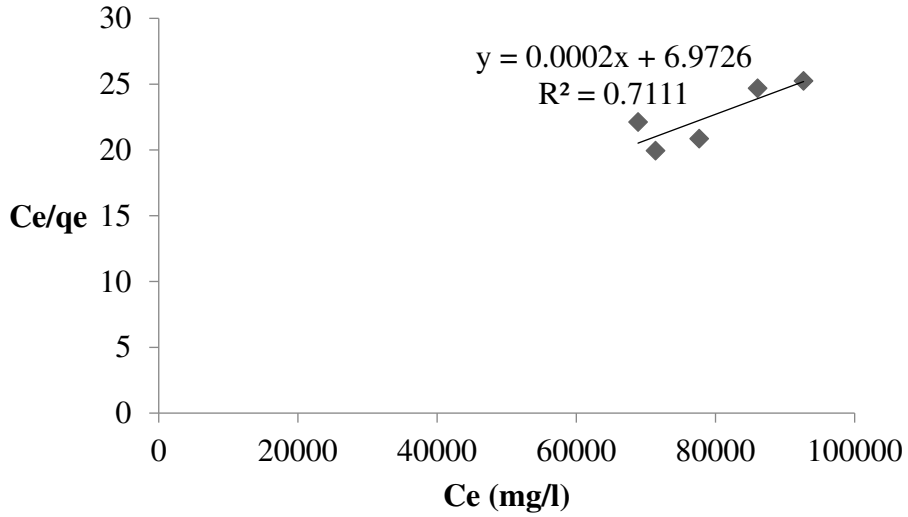

Figure 14: Langmuir isotherm for oil adsorption on raw AOBSP

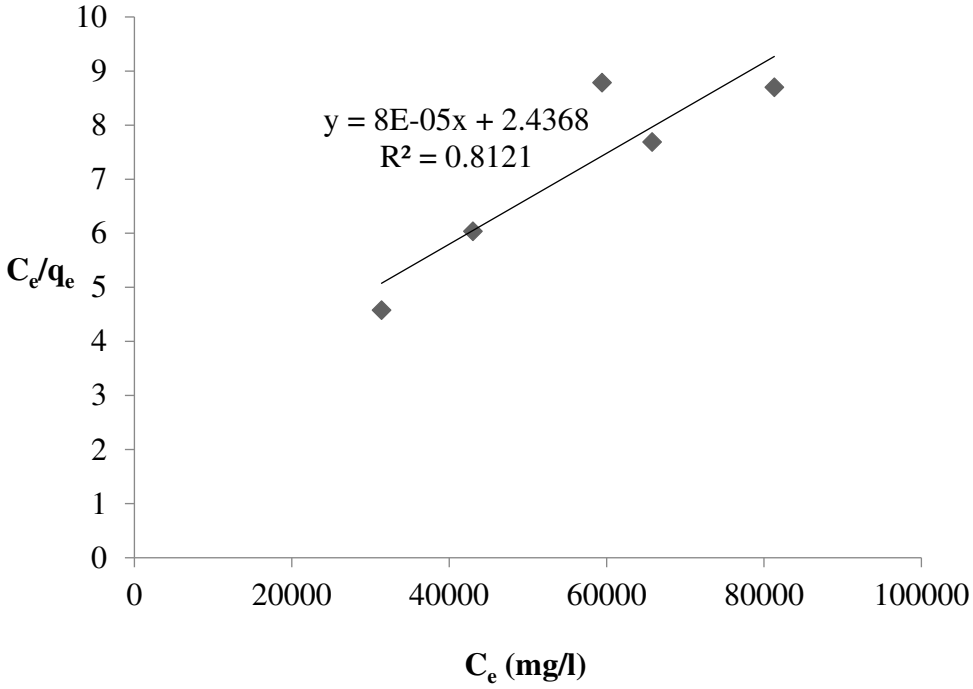

319

320 **Figure 15: Langmuir isotherm for oil adsorption on acetylated AOBSP**

321

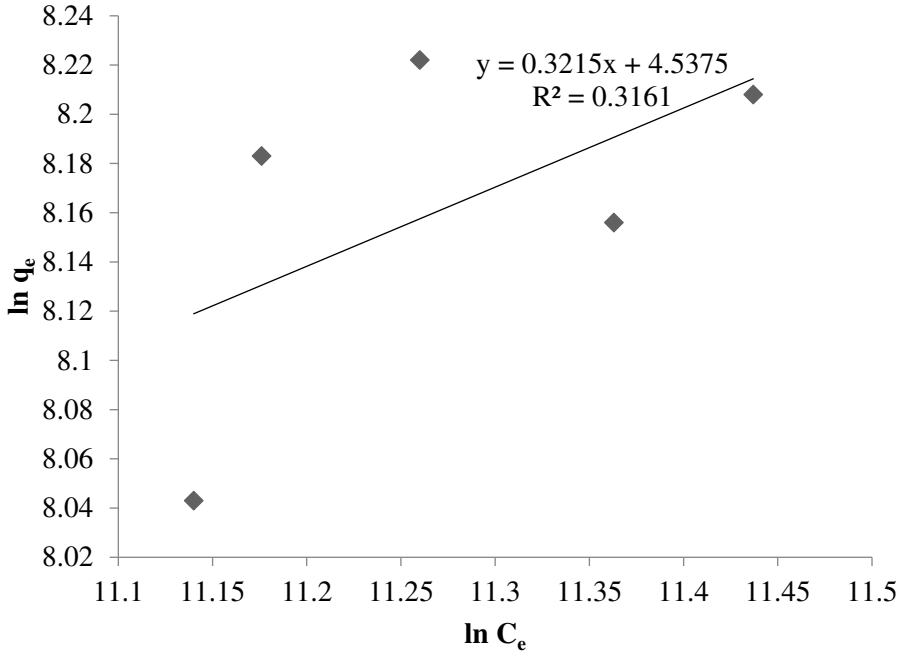

322

323 **Figure 16: Freundlich isotherm for oil adsorption on raw AOBSP**

324

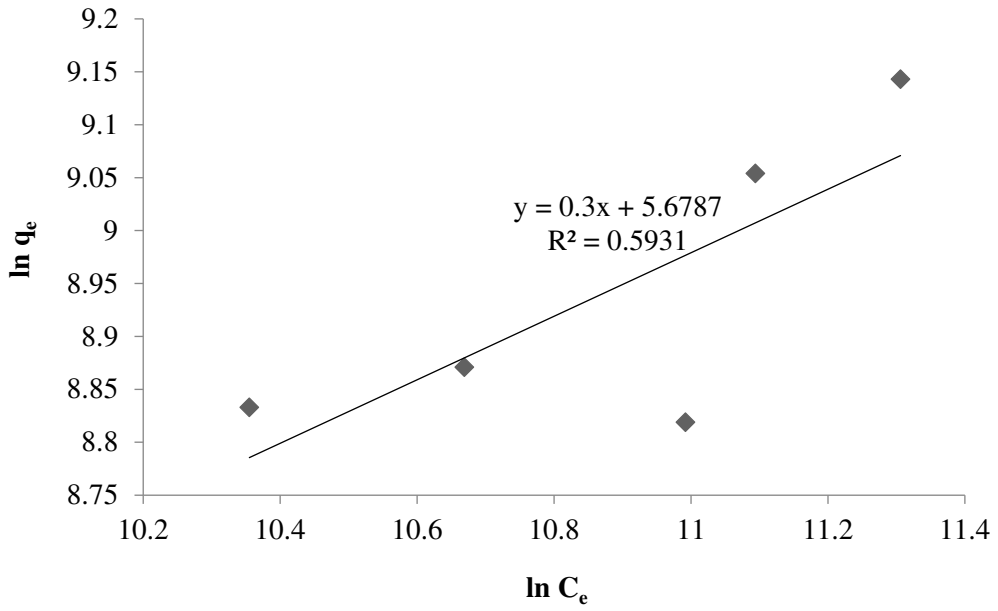

325

326 **Figure 17: Freundlich isotherm for oil adsorption on acetylated AOBSP**

327 The isotherm parameters for the crude oil adsorption on raw and acetylated AOBSP are shown in Table

328 5.

329 **Table 5: Isotherm parameters for oil adsorption on raw and acetylated AOBSP**

Parameter	**RAOBSP**	**AAOBSP**
Langmuir isotherm		
R^2	0.7111	0.8121
K_L (L/mg)	2.87 x 10^{-5}	3.28 x 10^{-4}
R_L	0.26	0.23
q_m (mg/g)	5000	12500
Freundlich isotherm		
R^2	0.3161	0.5931
K_F	93.457	292.57
n	3.11	3.33

For both RAOBSP and AAOBSP the R^2 values for Langmuir isotherm are higher than for Freundlich isotherm. This means that the adsorption of crude oil on both RAOBSP and AAOBSP are better described by Langmuir isotherm than Freundlich isotherm. This shows that oil adsorption on both RAOBSP and AAOBSP took place by monolayer coverage of the sorbents by the crude oil with no interaction between the adsorbed oil on adjacent sites (Mwangi et al. 2012). The K_L value for adsorption on AAOBSP (3.28×10^{-4} L/mg) is higher than the value for adsorption on RAOBSP (2.87×10^{-5} L/mg). This shows that there was greater affinity between the crude oil and AAOBSP than between the crude oil and RAOBSP. The R_L values were 0.26 and 0.23 for RAOBSP and AAOBSP, respectively. These values are between 0 and 1, thereby indicating the favourability of the adsorption of crude oil on both sorbents (Siswoyo et al. 2014). The monolayer sorption capacity was found to be 5000 mg/g for RAOBSP and 12500mg/g for AAOBSP, which shows the high improvement of the sorption capacity of AOBSP by acetylation. The sorption capacity of acetylated AOBSP is higher than some other reported acetylated lignocellulosic wastes, such as acetylated groundnut husk with sorption capacity of 9940mg/g (Chiaha et al. 2017) and acetylated oil palm empty fruit bunch fibre with sorption capacity of 10,000mg/g (Asadpour et al. 2016)

Thermodynamic studies

The results of thermodynamic analysis of crude oil adsorption on the raw and acetylated AOBSP are shown in Table 6.

352 **Table 6: Thermodynamic parameters for oil adsorption on raw and acetylated AOBSP**

Parameter	RAOBSP	AAOBSP
ΔG^o (kJ/mol)		
303K	-10.120	-12.031
308K	-10.093	-12.008
313K	-9.920	-11.996
318K	-9.148	-11.426
323K	-8.650	-10.365
ΔH^o (kJ/mol)	-33.906	-36.067
ΔS^o (kJ/mol)	-0.0777	-0.0783

353

354 For adsorption on both RAOBSP and AAOBSP, ΔG^o was found to have negative values at all the
355 considered adsorption temperatures, showing that adsorption on both RAOBSP and AAOBSP were
356 spontaneous and feasible and so did not require any external energy source (Adeogun et al. 2016).
357 Higher negative ΔG^o value shows a more energetically favorable adsorption (Kumar 2011). AAOBSP
358 was found to have higher negative ΔG^o values than RAOBSP at all the considered adsorption
359 temperatures showing that adsorption of crude oil on AAOBSP was more energetically favorable than
360 adsorption on RAOBSP. Also, lower negative ΔG^o values were obtained with increase in temperature,
361 showing that there was more efficient biosorption at lower temperature, which is supported by the
362 decrease in the value of sorption capacity of the sorbents with increase in temperature observed during
363 the study of effect of temperature on adsorption. The ΔH^o values were negative values, also confirming
364 that crude oil adsorption on both RAOBSP and AAOBSP were exothermic processes. The ΔS^o values
365 were found to be -0.0777kJ/mol and -0.0783kJ/mol for adsorption on RAOBSP and AAOBSP,

366 respectively. The negative value of ΔS^o shows that there was a reduction in randomness at the solid–
367 mixture interface during adsorption (Salisu et al. 2019). This is as a result of the adsorption of the oil
368 molecules to the sorbents' surfaces thereby leading to orderliness (Zhu et al. 2009). Also, according to
369 Nwosu et al. (2012), negative ΔS^o values show that the adsorption process did not result in any
370 significant change in the internal structure of the adsorbent. Thus, crude oil adsorption on both raw and
371 acetylated AOBSP was feasible, spontaneous, exothermic, and did not cause any significant change in
372 the internal structure of the adsorbent.

373 **CONCLUSION**

374 In this study, AOBSP, which is an agricultural waste, was found to be a suitable sorbent for crude oil
375 removal from aqueous solution. The sorption capacity increased substantially after acetylation. Crude
376 oil adsorption on both raw and acetylated AOBSP were spontaneous, exothermic, and did not cause
377 any significant change in the internal structure of the adsorbents. Adsorption on the raw pod was best
378 described by the pseudo first order kinetic model, while adsorption on the acetylated pod fitted best to
379 the pseudo second order model. Intra-particle diffusion also took part in controlling the rate of oil
380 sorption on both RAOBSP and AAOBSP. Adsorption on both raw and acetylated AOBSP took place
381 by monolayer coverage of the crude oil on the surface of the sorbents with the sorption capacity of the
382 raw and acetylated sorbents being 2500mg/g and 12500mg/g, respectively. Acetylated AOBSP is a
383 very promising alternative sorbent for crude oil spill mop because of its high sorption capacity and the
384 fact that AOBSP is readily available and a biodegradable waste.

385 **Abbreviations**

386 AOBSP: African oil bean seed pod; RAOBSP: raw African oil bean seed pod; AOBSP: acetylated
387 African oil bean seed pod; RAOBSP-S: raw African oil bean seed pod after crude oil sorption;
388 AAOBSP-S: acetylated African oil bean seed pod after crude oil sorption; API: American Petroleum

Institute; ATR: attenuated total reflection; ASTM: American Society for Testing and Materials; SEM: Scanning electron microscopy; BET: Brunauer, Emmett and Teller; BJH: Barrett, Joyner, and Halenda; DH: Dollimore and Heal; DR: Dubinin-Radushkevich; DFT: Density functional theory; HK: Horvath and Kawazoe; SF: Saito and Foley; DA: Dubinin-Astakhov; FTIR: Fourier-Transform Infrared; W_0: weight of adsorbent before oil adsorption; W_1: weight of adsorbent after oil adsorption; C_o: initial crude oil concentration (mg/L); C_e: equilibrium crude oil concentration (mg/L); m: mass of adsorbent (g); V: volume of solution (L); q_e: amount of adsorbate adsorbed at equilibrium (mg/g); q_t: amount of adsorbate adsorbed (mg/g); t: time (min); k_1: pseudo first order reaction rate constant (min^{-1}); k_2: pseudo-second order reaction rate constant (g/mg.min); K_{id}: rate constant of intraparticle diffusion ($mg/(g \cdot min^{0.5})$); K_L: Langmuir constant (L/mg); R_L: Langmuir separation factor; C_o: initial adsorbate concentration(mg/L); K_F: Freundlich constant [$(mg/g)/(mg/L)^{1/n}$]; n: measure of adsorption intensity; R: universal constant (8.314J/mol.K); T: absolute temperature (K); K_d: distribution coefficient for adsorption (cm^3/g); ΔG^o: standard Gibbs free energy change (kJ/mol); ΔH^o: change in enthalpy (kJ/mol); ΔS^o: change in entropy (kJ/mol.K).

DECLARATIONS

Ethics approval and consent to participate

Not applicable

Consent for publication

Not applicable

Availability of data and materials

All data generated or analysed during this study are included in this published article (and its supplementary information files).

Competing interests

The authors declare that they have no competing interests.

Funding

The work was funded by the authors.

Authors' contributions

AIO who is a doctoral candidate wrote the manuscript. VIA is the supervisor and provided comments and revisions to the manuscript. All authors read and approved the final manuscript.

Acknowledgement

Not applicable

REFERENCES

Adeogun AI, Idowu MA, Akiode KO, Ahmed SA (2016) Bioremediation of Cu(II) contaminated water by *Saccharum officinarum*: effect of oxalic acid modification on equilibrium, kinetic and thermodynamic parameters. Bioresour Bioprocess. 3:7. doi:10.1186/s40643-016-0085-9

Akinhanmi TF, Ofudje EA, Adeogun AI, Aina P, Joseph IM (2020) Orange peel as low-cost adsorbent in the elimination of Cd(II) ion: kinetics, isotherm, thermodynamic and optimization evaluations. Bioresour Bioprocess. 7:34. doi:10.1186/s40643-020-00320-y

Al-Dahhan WH, Mahmood SMA (2019) Classification of crude oils and its fractions on the basis of paraffinic, naphthenic and aromatics. Al-Nah J Sci 22(3):35-42. doi:10.22401/ANJS.22.3.05

Angelova D, Uzunov I, Uzunova, Gigova, Minchev, L (2011) Kinetics of oil and oil products adsorption by carbonized rice husks. Chem Eng J 172(1):306-311. doi:10.1016/j.cej.2011.05.114

433 Aningo JN, Chime TO, Nevo CO (2017) Adsorption of cadmium (II) ion from aqueous solution using
434 activated carbon from produced from oil been seed shell. J Multidis Eng Sci Tech 4(8):7993-8000.

435 Anuzyte E, Vaisis V (2018) Natural oil sorbents modification methods for hydrophobicity
436 improvement. Ene Proc 147:295-300. doi:10.1016/j.egypro.2018.07.095

437 Arinze-Nwosu UL, Ajiwe VIE, Okoye PAC, Nwadiogbu JO (2019) Kinetics and equilibrium of crude
438 oil sorption from aqueous solution using *Borassus aeothopum* coir. Chem Mat Res 11(2):12-19.
439 doi:10.7176/CMR

440 Asadpour R, Sapari NB, Isa MH, Kakooei S (2016) Acetylation of oil palm empty fruit bunch fiber as
441 an adsorbent for removal of crude oil. Environ Sci Pollut Res 23(12):11740-11750.
442 doi:10.1007/s11356-016-6349-2

443 Asadpour R, Sapari NB, Isa MH, Orji KU (2014). Enhancing the hydrophobicity of mangrove bark by
444 esterification for oil adsorption. Wat Sci Tech 70(7):1220-1228. doi:10.2166/wst.2014.355

445 Asadpour R, Sapari NB, Isa MH, Kakooei S, Orji KU (2015) Acetylation of corn silk and its application
446 for oil sorption. Fib Poly 16(9):1830-1835. doi:10.1007/s12221-015-4745-8

447 Awadh SM, Al-Mimar H (2015) Statistical analysis of the relations between API, specific gravity and
448 sulfur content in the universal crude oil. Int J Sci Res 4(5), 1279-1284.

449 Babarinde NAA, Babalola JOB (2010) The biosorption of Pb (II) from solution by elephant grass
450 (*Pennisetum purpureum*): kinetic, equilibrium, and thermodynamic studies. The Pacific Journal of
451 Science and Technology, 11(1), 622 – 630.

452 Barros FCDF, Vasconcellos LCG, Carvalho TV, Nascimento RFD (2014) Removal of petroleum spill
453 in water by chitin and chitosan. Orbital: Elec J Chem 6(1):70-74. doi: 10.17807/orbital.v6i1.509

454 Bodîrlău R, Teacă CA (2009) Fourier transform infrared spectroscopy and thermal analysis of
455 lignocellulose fillers treated with organic anhydrides. Rom Journ Phys 54(1-2):93-104.

456 Chiaha PN, Nwabueze HO, Ezekannagha CB, Okenwa CJ (2017) Kinetic studies on oil sorption using
457 acetylated sugarcane bagasse and groundnut husk. Int J Multidis Sci Eng, 8(6):16-21.

458 Dagde KK (2018). Biosorption of crude oil spill using groundnut husks and plantain peels as
459 adsorbents. Adv Chem Eng Sci 8:161-175. doi:10.4236/aces.2018.83011

460 El-Din GA, Amer AA, Malsh G, Hussein M (2018) Study on the use of banana peels for oil spill
461 removal. Alex Eng J 57:2061-2068. doi:10.1016/j.aej.2017.05.020

462 Erhan D, Mehmet K, Elif S, Tuncay O (2004) Adsorption kinetics for the removal of chromium (VI)
463 from aqueous solutions on the activated carbons prepared from agricultural wastes. Wat SA, 30(4):533-
464 541.

465 Gupta VK, Shrivastava AK, Jain N (2001) Biosorption of chromium (VI) from aqueous solutions by
466 green algae spirogyra species. Wat Res 35:4079-4090. doi:10.1016/s0043-1354(01)00138-5

467 Ho YS, McKay G (2000) The kinetics of sorption of divalent metal ions onto sphagnum moss peat.
468 Wat Res 34(3):735-742.

469 Idris S, Iyaka YA, Dauda BEN, Ndamitso MM, Umar MT (2012) Kinetic study of utilizing groundnut
470 shell as an adsorbent in removing chromium and nickel from dye effluent. Amer Chem Sci J 2(1):12-
471 24.

472 Ikirigo J, Sogbara F (2017) Perspective view on sorption thermodynamics: basic dye uptake on
473 southern Nigerian clay. Euro Sci J 13(18):355-372. doi:10.19044/ESJ.2017.V13N18P355

474 Karthikeyan G, Analagan K, Andal NM (2004) Adsorption dynamics and equilibrium studies of Zn
475 (II) onto chitosan. J Chem Sci 116(2):119-127.

476 Kudaybergenov, K.K., Ongarbayev, E.K. and Mansurov, Z.A. (2013) Petroleum sorption by thermally
477 treated rice husks derived from agricultural byproducts. Eura Chemico-Technol J 15:57-66.
478 doi:10.18321/ectj141

479 Kumar, U. (2011) Thermodynamics of the Adsorption of Cd (II) from Aqueous Solution on NCRH.
480 International J Environ Sci Dev 2(5):334-336. doi:10.7763/IJESD.2011.V2.147

481 Li Y, Hagos FM, Chen R, Qian H, Mo C, Di J, Gai X, Yang R, Pan G, Shan S (2021) Rice husk
482 hydrochars from metal chloride-assisted hydrothermal carbonization as biosorbents of organics
483 from aqueous solution. Bioresour Bioprocess 8:99. doi:10.1186/s40643-021-00451-w.

484 Li K, Zheng Z, Huang X, Zhao G, Feng J, Zhang J (2009) Equilibrium, kinetic and thermodynamic
485 studies on the adsorption of 2-nitroaniline onto activated carbon prepared from cotton stalk fiber. J Haz
486 Mat 166(1):213-220. doi:10.1016/j.jhazmat.2008.11.007

487 Madu AJC, Ugwu RE (2017). Physical and chemical properties of crude oils and their geologic
488 significances. Int J Sci Res 6(6):1514-1521.

489 Mahmoud MA (2020) Oil spill cleanup by waste flax fiber: modification effect, sorption isotherm,
490 kinetics and thermodynamics. Arab J Chem, 13:5553-5563. doi:10.1016/j.arabjc.2020.02.014

491 Mwangi IW, Ngila JC and Okonkwo JO (2012) A comparative study of modified and unmodified
492 maize tassels for the removal of selected trace metals in contaminated water. Tox Environ Chem 94:20-
493 39. doi:10.1080/02772248.2011.638636

494 Najaa-Syuhada MT, Rozidaini MG, Norhisyam I (2017). Response surface methodology optimization
495 of oil removal using banana peel as biosorbent. Malay J Anal Sci, 21(5), 1101 – 1110.
496 doi:10.17576/mjas-2017-2105-12

497 Nwabueze HO, Igbokwe PK, Amalu EU, Okoro SE (2015). A study on the equilibrium and kinetics of
498 oil spill cleanup using acetylated corncobs. Int J Environ Sci, 5(6):1106-1114.

499 Nwadiogbu JO, Ajiwe VIE, Okoye PAC (2016). Removal of crude oil from aqueous medium by
500 sorption on hydrophobic corncobs: Equilibrium and kinetic studies. J Taibah Univ Sci, 10, 56 – 63.
501 doi:10.1016/j.jtusci.2015.03.014

502 Nwosu FO, Olu-Owolabi BI, Adebowale KO (2012). Kinetics and thermodynamic adsorption of Pb
503 (II) and Cd (II) ions from used oil onto *Thevetia neriifolia* nutshell active carbon. Curr Res Chem
504 4(2):26-40. doi:10.3923/crc.2012.26.40

505 Nwosu, UC, Essien EB, Ohiri RC (2017). Phytochemical, mineral composition and anti-
506 hyperlipidemic effects of processed *Pentaclethra macrophylla* seeds on high fat diet and streptozocin-
507 induced diabetic wistar rats. Int J Agri Earth Sci 3(6):31-41. doi:10.9734/IJBCRR/2017/35235

508 Ofomaja AE, Ho Y (2007). Effect of pH on cadmium biosorption by coconut copra meal. J Haz Mat.
509 139(2), 356 – 362. doi:10.1016/j.jhazmat.2006.06.039

510 Okwunodulu FU, Odoemelam SA, Okon EN (2015). Biosorption of Cd^{2+}, Ni^{2+} and Pb^{2+} by the shell
511 of *Pentaclethra macrophylla*: equilibrium isotherm studies. J. Sci. Technol. Environ. Inform 2(1):26-
512 35. doi:10.18801/jstei.020115.13

513 Oloro J (2018). Effect of pH and API gravity on the water-in-oil emulsion stability. J Appl Sci Environ
514 Manage, 22(6):925-928. doi:10.4314/jasem.v22i6.14

515 Omer AM, Khalifa RE, Tamer TM, Ali AA, Ammar YA, Eldina MSM (2020) Kinetic and
516 thermodynamic studies for the sorptive removal of crude oil spills using a low-cost chitosan-poly (butyl
517 acrylate) grafted copolymer. Desal Water Treat 192:213-225. doi: 10.5004/dwt.2020.25704

518 Onwuka JC, Agbaji E, Ajibola VO, Okibe F (2016) Kinetic studies of surface modification of
519 lignocellulosic *Delonix regia* pods as sorbent for crude oil spill in water. J Appl Res Technol 14:415-
520 424. doi:10.1016/j.jart.2016.09.004

521 Onwuka JC, Agbaji E, Ajibola VO, Okibe F (2019) Thermodynamic pathway of lignocellulosic
522 acetylation process. BMC Chem, 13:79-90. doi:10.1186/s13065-019-0593-8

523 Onwuka JC, Agbaji E, Ajibola VO, Okibe F (2018) Treatment of crude oil-contaminated water
524 with chemically modified natural fiber. Appl Water Sci 8(86):1-10. doi:10.1007/s13201-018-0727-5

525 Santos CM, Dweck J, Viotto RS, Rosa AH, de Morais LC (2015) Application of orange peel waste in
526 the production of biofuels and biosorbents. Biores Tech 196:469-479.
527 doi:10.1016/j.biortech.2015.07.114

528 Shah AJ, Soni B, Karmee SK (2021) Locally available agroresidues as potential sorbents: modelling,
529 column studies and scale-up. Bioresour Bioprocess. 8:34. doi:10.1186/s40643-021-00387-1

530 Shittu TD, Aransiola EF, Alabi-Babalola OD (2020). Adsorption performance of modified sponge
531 gourd for crude oil removal. J Environ Protect, 11:65-81. doi:10.4236/jep.2020.112006

532 Shweta S, Jha H (2016) Synthesis and characterization of crystalline carboxymethylated lignin – TEOS
533 nanocomposites for metal adsorption and antibacterial activity. Bioresour Bioprocess 3:31. doi:
534 10.1186/s40643-016-0107-7

535 Simonivić BR, Aranđelović D, Jovanović M, Kovačević B, Pezo L, Jovanović A (2009). Removal of
536 mineral oil and wastewater pollutants using hard coal. Chem Ind Chem Eng Q 15(2):57-62.
537 doi:10.2298/CICEQ0902057S

538 Teli MD, Valia SP (2016) Effect of substrate geometry on oil sorption capacity of raw and chemically
539 modified jute fibre. IRA-Int J Technol Eng 3(3):138-147. doi:10.21013/jte.v3.n3.p4

540 Thompson NE, Emmanuel GC, George NI, Adamu IK (2015) Modelling of the kinetic and equilibrium
541 sorption behaviour of crude oil on HDTMAB modified Nigerian nanoclays. Int J Sci Technol 4(2):106-
542 114.

543 Wali E, Nwankwoala HO, Ocheje JF, Onyishi CJ (2019) Oil spill incidents and wetlands loss in Niger
544 delta: implication for sustainable development goals. Int J Environ Poll Res 7(1):1-20.

545 Xu Y, Yang H, Zang D, Zhou Y, Liu F, Huang X, Chang J, Wang C, Ho S (2018) Preparation of a new
546 superhydrophobic/ superoleophilic corn straw fiber used as an oil absorbent for selective absorption of
547 oil from water. Bioresour Bioprocess 5:8. doi:10.1186/s40643-018-0194-8

548 Yasin G, Bhanger MI, Ansari TM, Naqvi SMSR, Ashraf M, Ahmad K, Talpur FN (2013). Quality and
549 chemistry of crude oils. J Pet Technol Alt Fuels 4(3):53-63.

550 Zhu C, Wang L, Chen W (2009) Removal of Cu(II) from aqueous solution by agricultural by-product:
551 peanut hull. J Haz Mat 168:739-746.

552

553

554

555

556 **Table 2: Surface area measurements of African oil bean seed pod (AOBSP)**

Measurement	Raw AOBSP	Acetylated AOBSP
Surface area (m^2/g)		
SinglePoint BET	137.7	192.0
MultiPoint BET	226.4	310.0
Langmuir surface area	1358	1620
BJH method cumulative adsorption surface area	255.1	355.1
DH method cumulative adsorption surface area	271.3	378.3
t-method external surface area	226.4	310.0
DR method micropore area	242.4	335.8
DFT cumulative surface area	53.93	74.76
Pore volume (cc/g)		
BJH method cumulative adsorption pore volume	0.1254	0.1741
DH method cumulative adsorption pore volume	0.1283	0.1783
DR method micropore volume	0.0861	0.1193
HK method micropore volume	0.0359	0.0505
SF method micropore volume	0.0074	0.0108
DFT method cumulative pore volume	0.0652	0.0895
Pore size (nm)		
BJH method adsorption pore diameter	2.123	2.131
DH method adsorption pore diameter	2.123	2.131
DR method micropore width	6.247	6.181
DA method pore diameter	2.940	2.920

HK method pore diameter	1.847	1.847	557
SF method pore diameter	3.497	3.488	
DFT pore diameter	2.647	2.647	

Supplementary Files

This is a list of supplementary files associated with this preprint. Click to download.

- ADDITIONALFILES.docx
- GRAPHICALABSTRACT.jpg